Scientific African 16 (2022) e01188

Contents lists available at ScienceDirect

Scientific African

journal homepage: www.elsevier.com/locate/sciaf

Synthesis of N, N(1,3-phenylene)dimethanimine: A useful resource for the removal of free fatty acid in waste vegetable oil

Titilope R. Ushedo[a], Olalere G Adeyemi[a], Adewale Adewuyi[a,*], Woei J Lau[b]

[a] Department of Chemical Sciences, Faculty of Natural Sciences, Redeemer's University, Ede, Osun State, Nigeria
[b] Advanced Membrane Technology Research Centre (AMTEC), School of Chemical and Energy Engineering, Universiti Teknologi Malaysia, Skudai, Johor 81310, Malaysia

ARTICLE INFO

Article history:
Received 20 October 2020
Revised 26 March 2022
Accepted 4 April 2022

Editor: DR B Gyampoh

Keywords:
Adsorption
DFT
FFA
Langmuir
Vegetable oil

ABSTRACT

Developing an efficient material for the removal of free fatty acids (FFAs) in waste vegetable oil is a challenge in the refining of vegetable oil in food and oleochemical industries. In response to this, N,N(1, 3-phenylene)dimethanimine (NPD) was synthesized via green reaction route without involving solvent. NPD was characterized using Fourier transformed infrared spectroscopy (FTIR), X-ray diffraction (XRD), transmission electron microscopy (TEM), thermogravimetric (TG) analysis, scanning electron microscopy (SEM), and energy-dispersive X-ray spectroscopy (EDX). NPD was then applied as a material for the removal of FFA from waste cooking oil (WCO). The synthesis process gave a high yield of 95% of NPD. The FTIR result revealed different functional groups in NPD; the TG showed mass loss at diverse temperature range revealing loss at 80–150, 180–250, 250–410 and 410–600 °C while loss above 600 °C was assigned to loss of char. while TEM revealed the surface of NPD to be smooth with an irregular shape. EDX results further demonstrated the presence of oxygen, nitrogen and carbon in NPD. Removal of FFA from WCO may be described by pseudo-second-order with an adsorption capacity of 42.30 L kg^{-1}. The process obeyed Langmuir isotherm with ΔH of -0.679 kJ mol^{-1} and ΔS of -0.049 kJ mol^{-1} K^{-1} while ΔG increased with increase in temperature. The Density Functional Theory (DFT) concept was used to explain the action of NPD as an adsorbent with the aid of lowest unoccupied molecular orbital (LUMO) and the highest occupied molecular orbital (HOMO). It revealed the mechanism of removal of FFA from WCO by NPD to be via nucleophilic interaction.

Introduction

Vegetable oils can serve as cooking and in most cases are used for frying other food and food materials. When used for frying, they lose value due to deep processing as they undergo chemical degradation, leading to the formation of molecules

* Corresponding author.
E-mail address: walexy62@yahoo.com (A. Adewuyi).

https://doi.org/10.1016/j.sciaf.2022.e01188

such as oxides, higher oxides and free fatty acids [1,2]. The formation of these molecules is undesirable and may have to be removed from vegetable oil when formed. Vegetable oils containing undesired amount of any of these molecules are considered as waste cooking oil (WCO). The main compositions of WCO have been reported to be free fatty acids (FFAs) and glycerides [3,4].

Large amount of WCOs is generated globally due to domestic activities [5,6]. It is a major challenge in most developing countries of the world, such as those in the African region. Currently, Nigeria and other countries of the world are faced with this problem, and it is challenging to find the most suitable means of reusing such WCOs. The challenge is not just the generation of WCOs, but the handling and adequate disposal of the WCOs are much more difficulties. Inadequate disposal has led to the contamination of soil and water with WCOs, which is a severe environmental issue [7]. Although cooking oil is biodegradable, but this takes time and may become expensive if an enhanced biodegradable process is employed. However, it is better to find alternative use of these WCOs instead of ejecting them into the environment. One of these possibilities will be to refine them for reuse or treat them to meet the specification for other possible applications either as direct use or as feedstocks for other products [8]. One of such applications may include their use as feedstock for biodiesel production. Moreover, currently one of the main uses of WCOs is as a raw material for the biodiesel production.

WCOs can be refined to become useful [9]. The refining process involves the removal of undesired components such as colours, FFA, peroxides, phospholipids, metals, flavours and other higher oxides [10]. These refining processes may include degumming, bleaching, chemical neutralization, distillation and deodorization [11–13]. Some of the refining processes have shortcomings like being expensive and incomplete removal of the undesired components in WCO. The removal of FFA from WCO is mostly achieved via neutralization using an alkaline solution. Most times, this leads to the formation of soap [14], which may cause difficulty during the separation of the refined oil from process impurities, especially when sodium carbonate (Na_2CO_3) is used as chemicals for refining WCO. This process might also lead to the saponification of a little amount of triglyceride, resulting in loss of oil. The use of chemicals to reduce FFA may not be considered as a green process, which necessitates the need for a process that is sustainable, cheap and green. Currently, adsorption is used as a process for the removal of contaminants in solution. Previous studies have reported the use of different types of adsorbents for the removal of FFA, some of these adsorbents includes, natural and activated zeolite [15], SiO_2/MgO [16], trisyl commercial silicas [17], modified potato and cassava starch [18], commercialized resin [19], and Cameroonian clay [20]. The use of adsorption process comes with several advantages such as affordability, ease of removal, reusability of adsorbent over time, and recovery of adsorbate without being deformed. Due to the uniqueness and ease of operation, this study proposes the use of an imine as adsorbents for the removal of FFA from WCO.

The imine is an organic compound containing a carbon-nitrogen double bond. It can be referred to as a Schiff base depending on the substituents on the nitrogen atom. Previous studies have shown that FFA can interact with the surface of adsorbent with its carboxylic functional group so that it adsorbs on the surface of such adsorbent [21,22]. The imine is capable of undergoing reaction with the lone-pair of electron on its nitrogen atom, which may include nucleophilic interaction. Such interaction may become feasible in the case of FFA in WCO. To this end, this study synthesized N, N(1, 3-phenylene)dimethanimine (NPD) (an imine) via the green reaction route. It was achieved in a solventless system making use of a melt-phase reaction that involved the reaction between *n*-phenylenediamine and formaldehyde. The NPD produced was used as an adsorbent for the removal of FFA in WCO.

Experimental

Materials

Groundnut oil (GO), also known as *Arachis hypogaea*, was purchased from a market in Osogbo, Osun State, Nigeria. The fatty acid composition has been reported to be dominantly oleic and linoleic fatty acids which ranged from 55.47 to 62.93% and 19.56 to 24.01%, respectively [23,24]. Formaldehyde, *n*-phenylenediamine, chloroform, methanol, hexane, diethylether and NaOH were purchased from Aldrich Chemical Co., England. GO was used for deep frying until it became deteriorated with FFA value reaching 50 g kg^{-1} to become WCO. The FFA value was determined by titrating the oil with 0.1 M NaOH using phenolphthalein as indicator.

Preparation of NPD

NPD was prepared via melt-phase (solventless) reaction between *n*-phenylenediamine and formaldehyde in a ratio 1:2. N- phenylenediamine (1 mol) was mixed with formaldehyde (2 mol) at 90 °C in a crucible and stirred continuously using a temperature-controlled magnetic stirrer for 30 min. It was allowed to cool while a brown product was formed with a yield of 95%. The scheme for the reaction is presented in **Fig. SM1**.

Characterization of NPD

The functional groups in NPD were determined using FTIR (FTIR, Perkin Elmer, spectrum RXI 83,303, MA, USA); values were recorded in the range of 400–4500 cm^{-1}. The X-ray diffraction pattern of NPD was measured using X-ray diffractometer (Smartlab, Rigaku) at a scanning speed, range and step width of 8.255° min^{-1}, 3.000–100.000° (2θ) and 0.020°,

respectively with filtered Cu Kβ radiation operated at 40 kV and 30 mA. TG analysis was carried out using TGA Q500 V20. Surface morphology of NPD was examined on TEM (HT7700, Hitachi). In order to confirm the elemental composition, SEM equipped with EDX detector (TM3000, Hitachi) was used.

Adsorption of FFA using NPD

Adsorption of FFA from WCO was studied by contacting 50 mL of WCO with 0.1 g of NPD in a 100 mL Erlenmeyer flask while stirring continuously for 120 min. As the stirring progressed, WCO was intermittently withdrawn and analyzed for FFA content by titrating with 0.1 M NaOH using phenolphthalein as indicator. An initial concentration range of 30–50 g kg^{-1} FFA content was used. The process was repeated by varying the weight of NPD in the range of 0.1–0.5 g and at different temperatures, which ranged from 25 to 50 °C.

Desorption studies

The desorption study was carried out in the presence of water, chloroform, methanol, hexane, ethylacetate, diethyl ether and chloroform/methanol (1:2). This was achieved by contacting 0.1 g of NPD with WCO having an initial concentration of 50 g kg^{-1} FFA in 100 mL Erlenmeyer's flasks at room temperature while stirring continuously for 120 min. The FFA loaded NPD was dried at room temperature for 48 h. In order to determine the desorption capacity, FFA loaded NPD were separately poured into different 250 mL Erlenmeyer's flasks containing 100 mL of the solvent (water, chloroform, methanol, hexane, ethylacetate, chloroform/methanol (1:2) or diethylether). These were stirred continuously at room temperature for 120 min. The amount of FFA desorbed was determined by titrating with 0.1 M NaOH using phenolphthalein as indicator. Desorption of FFA from NPD was calculated as:

$$Desorption\ (\%) = \frac{q_e(desorption)}{q_e(adsorption)} \times 100 \quad (1)$$

Quantum chemical parameters

The removal of FFA by NPD was theoretical explained using the DFT electronic structure programs at B3LYP/6–31 G level theory (Spartan 14.1 software). The molecular electronic structure of NPD was modelled, including the distribution of frontier molecular orbitals to establish the interaction of NPD with FFA.

Results and discussion

Preparation and characterization of NPD

Preparation of NPD was monitored using FTIR. The FTIR result is presented in **Fig. 1(a)**. The FTIR revelled peaks at 3428 and 3382 cm^{-1}, which were attributed to the N–H stretching of imine. A signal for C–H stretch was seen at 2832 cm^{-1} while the band seen at 1628 cm^{-1} was attributed to N–H bending frequency. The result further revealed a band at 1538 cm^{-1} which was attributed to the C=C stretching of an aromatic ring. The appearance of the band at 792 cm^{-1} was attributed to the wagging frequency while the peak at 1385 cm^{-1} was assigned to the frequency of C–N stretching of imine. The XRD result shown in **Fig. 1(b)** describes the diffraction pattern of NPD. The broadening of the XRD peaks at different plane values shows that the molecule of NPD has small size [25]. The TG and TEM image of NPD is shown in **Fig. 1(c) and (d)**, respectively. The thermogravimetric analysis revealed mass loss. The loss between 80 and 150 °C was attributed to evaporation of the adsorbed water molecules. Another loss was observed at 180–250 °C as well as at 250–410 °C. A loss noticed from 410 to 600 °C was attributed to the loss of aromatic molecules while loss above 600 °C was assigned to loss of char. The TEM image revealed a smooth surface with an irregular shape. The surface mapping for EDX is shown in **Fig. 2**. It revealed the presence of oxygen, nitrogen and carbon in the molecule of NPD.

Adsorption of FFA using NPD

The ability of NPD to remove FFA from WCO over a contact period was studied at 25 and 50 g kg^{-1} of WCO; the results are presented in **Fig. 3a**. A complete removal (100%) was achieved at a period of 120 min. The complete removal of FFA by NPD revealed its superior performance when compared to previously reported adsorbents like natural and activated zeolite, commercialized resin, and Cameroonian clay [18–20]. The complete removal also showed that NPD is better than activated carbon-based bio-adsorbents from pineapple dregs, bagasse, and coconut husk [26]. This relatively short time of removal suggests that the process may likely be described via kinetic [27]. The removal of FFA increased over time. The removal of FFA was found to increase with the amount of NPD used. Weight of NPD ranging from 0.1 to 0.5 g, was used for the removal of FFA. The removal of FFA was high for the first 10 min as the weight of NPD increased (0.1 to 0.5 g). The observation might be because the rate of chemical reaction increases with an increase in active surface area. The increase in weight of NPD must have made more active surface area available for the interaction between NPD and FFA. The observed high percentage

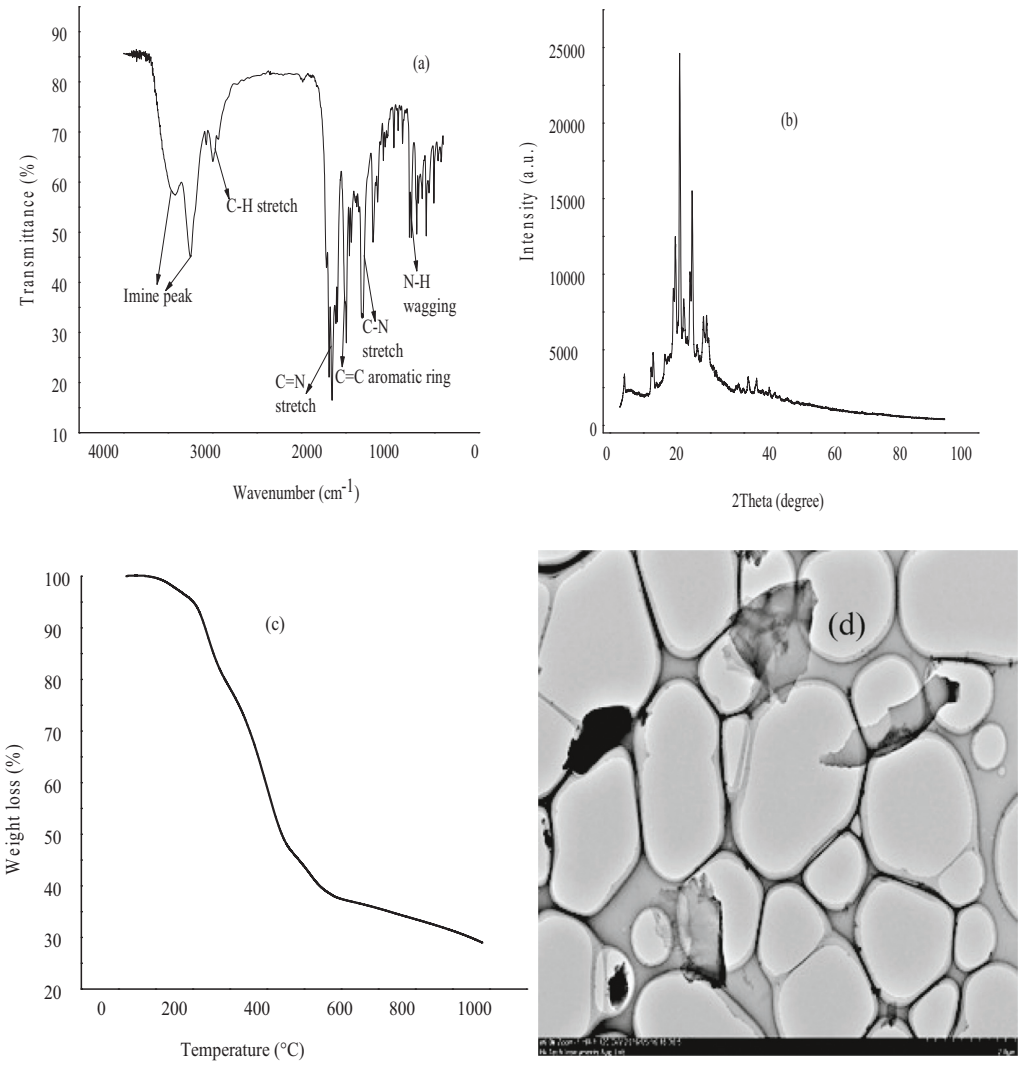

Fig. 1. FTIR (a), XRD (b), TG analysis (c) and TEM image (d) of NPD.

removal of FFA by NPD suggests NPD as a potential resource for the removal of FFA in waste vegetable oil. The adsorption capacity of NPD towards FFA is shown in **Fig. 3b**. The capacity of NPD to adsorb FFA was calculated using the following equation:

$$q_e = \frac{(C_o - C_e)V}{M} \tag{2}$$

where q_e is the adsorption capacity of NPD in L kg^{-1}, C_o and C_e are initial and final amounts of FFA in g kg^{-1}, respectively, V is the volumes (L) of treated oil and M is the weight (g) of NPD. The adsorption capacity of NPD towards FFA was found to be 42.30 L kg^{-1}. Furthermore, the adsorption capacity expressed by NPD toward FFA increased as the experimental time increased. On the contrary, the adsorption capacity reduced as the weight of NPD increased. This observation might be due to an ineffective mass transfer of FFA over NPD as the weight of NPD increased. Despite the reduction in adsorption capacity, the percentage removal of FFA increased which may be due to increase in active surface area as weight of NPD increased.

Adsorption kinetics

Removal of FFA by NPD was kinetically studied by fitting the experimental data with Elovich, intra-particle diffusion, pseudo-first-order and pseudo-second-order models. The linearized form of the pseudo-first-order rate equation is as follows [28]:

$$Ln(q_e - q_t) = Lnq_e - k_1 t \tag{3}$$

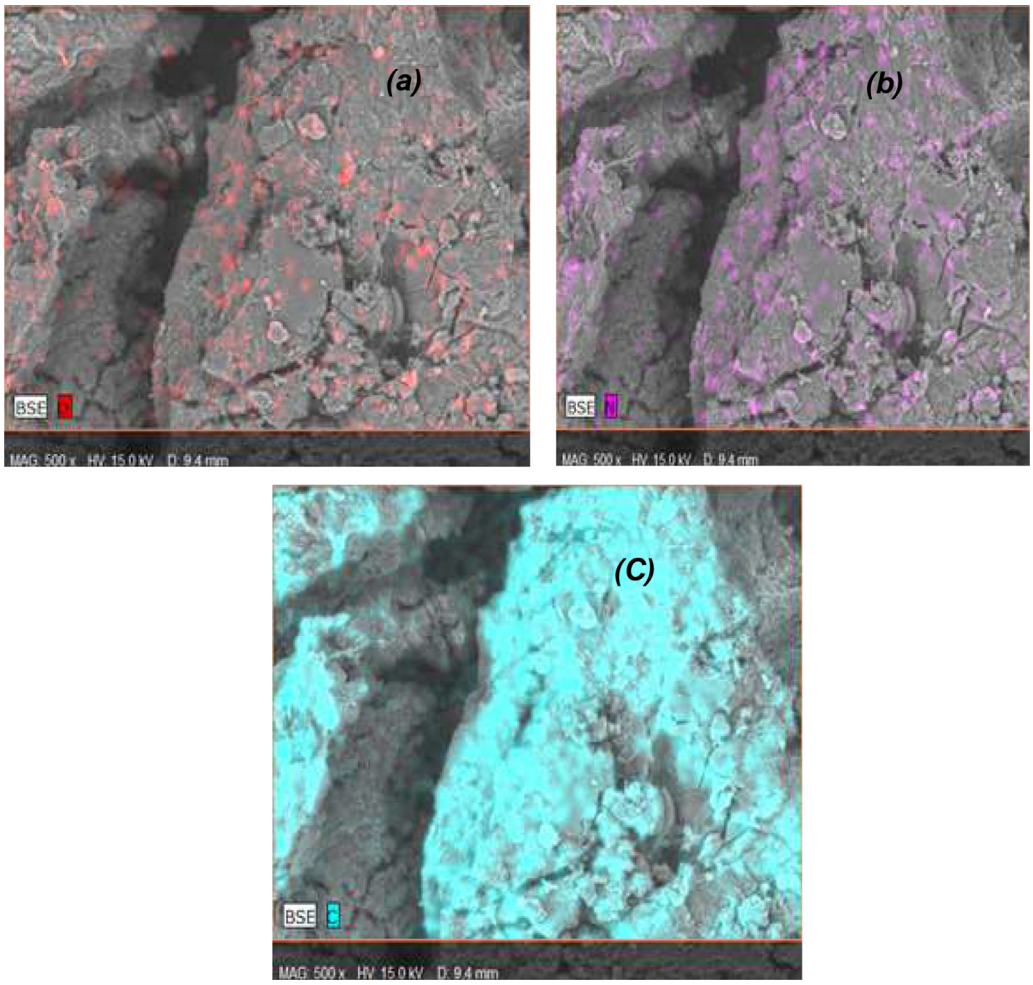

Fig 2. EDX surface analysis of NPD with respect to oxygen (a), nitrogen (b) and carbon (c).

Table 1
Kinetic model parameters for the sorption of FFA on NPD.

Model	Parameter	NPD
Pseudo-First-order	q_e (L kg^{-1})k_1 (min^{-1})r^2	1.390.020.83
Pseudo-second-order	q_e (L kg^{-1})k_2 (L kg^{-1} min^{-1})r^2h (L kg^{-1} min)	42.506.62 × 10^{-05}0.990.26
Elovich	β (L kg^{-1})α (L kg^{-1} min^{-1})r^2	15.392.480.77
Intra-particle diffusion	k_{id} (L kg^{-1} $min^{1/2}$)C (L kg^{-1})r^2	7.3533.000.92
Experiment	q_e (L kg^{-1})	42.30

where t is time, q_e and q_t represents amounts of FFA at equilibrium and time t, respectively, while k_1 represents the pseudo-first-order rate constant (min^{-1}). Ln(q_e-q_t) was plotted against t from which k_1 and q_e were obtained from the intercept and slope of the plot. As shown in **Table 1**. The data did not fit well for pseudo-first-order owing to the low r^2 value obtained (0.83). However, data were further subjected to the linearized form of the pseudo-second-order, which is given as [29]:

$$\frac{t}{q_t} = \frac{1}{k_2 q_e^2} + \frac{t}{q_e} \tag{4}$$

From Eq. (4), k_2 (L kg^{-1} min^{-1}) represents the adsorption rate constant. The q_e and k_2 were obtained from the slope and intercept of the plot of t/qt versus t while the initial sorption capacity (L kg^{-1} min), ho, was obtained from:

$$h_o = k_2 q_e^2 \tag{5}$$

The data fitted best for pseudo-second-order with better regression coefficients when compared to the other models studied. The q_e for the pseudo-second-order was found to be 42.50 L kg^{-1}, this value is close to the value (42.30 L kg^{-1}) obtained from the experimental data. It affirms the fact that the pseudo-second-order model best describes the removal

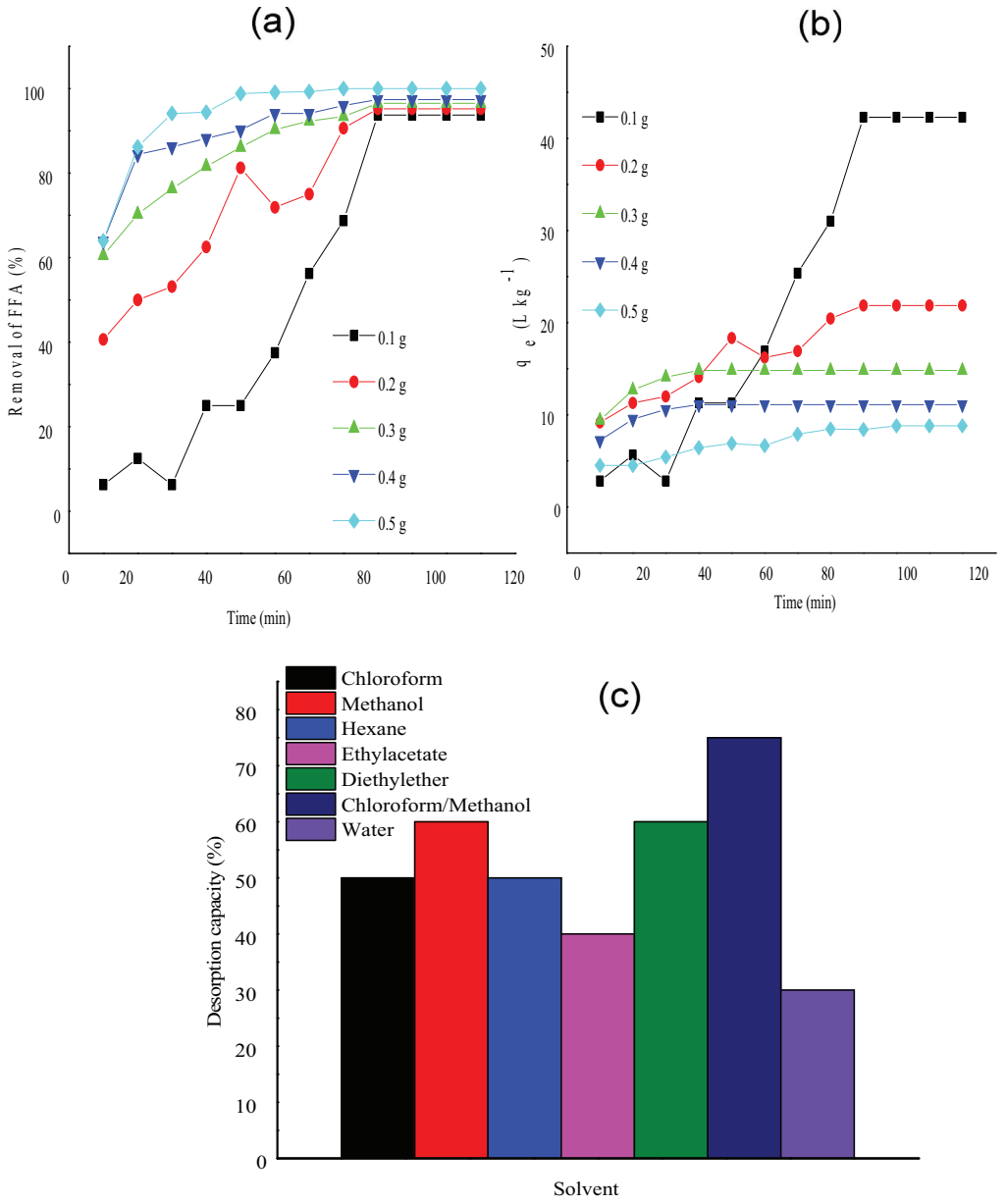

Fig. 3. (a) Percentage removal of FFA by NPD at varying weight at 25 °C and 50 g kg^{-1} of WCO, (b) Adsorption capacity of NPD towards FFA at varying weight at 25 °C and 50 g kg^{-1} of WCO and (c) Desorption capacity of NPD towards FFA using different solvents.

process, which suggests the removal process as a rate controlled, indicating a chemisorption process [30]. Data were also fitted for Elovich to model the process further. The linear expression of the model can be written as:

$$q_t = \frac{1}{\beta} Ln\,(\alpha\beta) + \frac{1}{\beta} Ln\, t \tag{6}$$

α is the initial adsorption rate (L kg^{-1} min), and β is the extent of surface coverage (L kg^{-1}). A plot of q_t vs Ln t did not fit well with a poor r^2 of 0.77. However, β was calculated from the slope of $(1/\beta)$, and α was estimated from the intercept of $1/\beta$ $Ln(\alpha\beta)$. Intra-particle diffusion was considered as a model in order to study the rate-limiting step for the removal of FFA by NPD, which was expressed as:

$$q_t = K_{id} t^{0.5} + C \tag{7}$$

From the expression, C (L kg^{-1}) is a constant, which shows the boundary layer thickness while the k_{id} is the intra-particle diffusion rate constant (L kg^{-1} $min^{-1/2}$). The fitting of the data gave a straight line with an r^2 value of 0.92 from the graph

Table 2
FFA sorption parameters for Langmuir and Temkin models.

Parameter	NPD
Langmuir	
Q_o (L kg^{-1})	42.372
K_L (L mg^{-1})	78.667
r^2	0.999
R_L	0.005
Temkin	
A (L g^{-1})	3.910
B (J mol^{-1})	26.112
r^2	0.978

of q_t versus $t^{1/2}$. The values obtained for C and K_{id} are presented in **Table 1**. The model suggests that the removal process was influenced by intra-particle diffusion. It became clear that the process is chemically rate controlled with the influence of intra-particle diffusion.

Isotherms

Data generated were fitted for three different isotherm models, which are Langmuir, Temkin, and Freundlich models. The data fitted best for Langmuir isotherm when compared with the two other isotherm models considered. The linear expression for the Langmuir isotherm model can be described as:

$$\frac{C_e}{q_e} = \frac{1}{Q_o}C_e + \frac{1}{K_L}Q_o \tag{8}$$

The equilibrium amount of FFA is represented as C_e (g kg^{-1}), q_e (L kg^{-1}) represents the amount of FFA removed at equilibrium, Q_o (L kg^{-1}) is the maximum monolayer coverage capacity, and K_L (L mg^{-1}) represents the Langmuir isotherm constant. When C_e/q_e was plotted against C_e, a straight line was obtained having a slope of $1/Q_o$ and an intercept of $1/Q_oK_L$ where K_L represents the essential features of the Langmuir isotherm, which is given as:

$$R_L = \frac{1}{1 + (1 + K_L C_o)} \tag{9}$$

From Eq. (9), C_o is the initial amount of FFA while K_L relates to the energy of sorption of FFA. Values of R_L may be interpreted as, when $R_L = 1$, sorption process is considered to be linear, when $R_L > 1$ sorption process is considered to be unfavourable when $0 < R_L < 1$, the process is considered to be favoured and irreversible if $R_L = 0$. With Langmuir, the process assumes uniform energy of adsorption at the surface of NPD and a monolayer coverage. The removal of FFA by NPD falls within $0 < R_L < 1$ as shown in **Table 2** indicating that the process is Langmuir isotherm favoured, the sorption energy is uniform and the covering of the surface of NPD by FFA is monolayered. The Q_o was found to be 42.372 L kg^{-1} with an r^2 value of 0.999. The data did not fit well for Freundlich isotherm; however, data were further subjected to Temkin isotherm as follows.

$$q_e = \left(\frac{RT}{b}\right) Ln(AC_e) \tag{10}$$

$$q_e = BLnA + BLnC_e \tag{11}$$

This isotherm is characterized by a uniform distribution of the binding energies up to some maximum binding energy due to adsorbent-adsorbate interactions. From the expression, A (L g^{-1}) represents Temkin isotherm equilibrium binding constant, B (J mol^{-1}) = RT/b and *b* is the Temkin constant. *T* (K) represents the absolute temperature and *R* (8.314 J mol^{-1} K) is the gas constant. On plotting q_e against Ln C_e a straight line with r^2 value of 0.978 was obtained from which B and A were determined from the slope and intercept.

Thermodynamics for the sorption of FFA by NPD

The removal of FFA by NPD was subject to thermodynamic evaluation by determining parameters such as Gibb's free energy change (ΔG^o), enthalpy change (ΔH^o) and entropy change (ΔS^o). Adsorption equilibrium constant b_o was estimated as [31]:

$$b_o = \frac{C_e}{C_o} \tag{12}$$

$$\Delta G^o = -RTLnb_o \tag{13}$$

$$\Delta G^o = \Delta H^o - T\Delta S^o \tag{14}$$

Table 3
ΔG, percentage removal and q_e obtained at various temperatures for removal of FFA by NPD.

T (K)	303	308	313	318	323
q_e (L kg^{-1})	43.42	43.92	44.12	44.22	44.62
Removal (%)	96.23	97.34	97.78	98.00	98.89
ΔG (kJ $mol^{-1}K^{-1}$)	8.16	9.22	9.85	10.29	12.06

In Eq. (12), C_o and C_e represent initial and equilibrium amount of FFA. In Eq. (13), *R* represents the universal gas constant (8.314 J mol^{-1} K^{-1}) while *T* (K) is the absolute temperature. On plotting Ln b_o against reciprocal of temperature (1/T), a straight line was obtained from which ΔH^o and ΔS^o were determined from the slope and intercept. The values for ΔG^o and qe obtained at different temperatures are presented in **Table 3**. The temperature ranged from 303 to 323 K. The ΔG^o increased from 8.16 to 12.06 kJ mol^{-1} K^{-1} as the temperature increased from 303 to 323 K. The percentage removal and qe also increased with temperature. The positive nature of the values obtained for ΔG^o is an indication that the process is non-spontaneous. Both ΔH^o (−0.679 kJ mol^{-1}) and ΔS^o (−0.049 kJ mol^{-1} K^{-1}) were found negative. The negative value of ΔH^o is an indication that the process is exothermic while the negative nature of ΔS^o indicates that the process is well ordered suggesting a stable configuration of FFA on the surface of NPD.

Desorption

The desorption of FFA from the surface of NPD was studied to evaluate the reusability of NPD. This also gave an idea of the regeneration of NPD for further removal of FFA. This was achieved using different solvent systems. The solvents used was based on the solubility of fatty acids. Results obtained for the percentage desorption is presented in **Fig. 3c**. The highest desorption of 75% was found for the mixture of chloroform/methanol (1:2). The previous study has reported that this is a good solvent mixture for the extraction of total lipids [32]. The lowest desorption was obtained when distilled water (30%) was used. This has shown that apart from the removal of FFA from used vegetable oil, the FFA can be recovered for reuse while the NPD is also regenerated for reuse. The current study has shown that NPD can be used for the removal of FFA from waste vegetable while NPD is regenerated using chloroform/methanol (1:2).

Quantum chemical computations and adsorption mechanism

The removal of FFA from WCO by adsorption may be due to the chemical interaction between the surface of NPD and FFA. However, FFA may have interacted with the surface of NPD as described in **Fig. SM2**. The formation of ammonium carboxylate may also be responsible for the inability to attain a 100% desorption capacity for NPD since the carboxylate ion has low reactivity towards nucleophilic addition or elimination, which limits further reaction in solution. However, a 75% desorption capacity was obtained.

DFT was performed at B3LYP/6–31 G level theory using Spartan 14.1 software as previously described [33]. The electronic properties of NPD are shown in **Fig. SM3**. It covers the optimized geometry, HOMO and LUMO density distribution, electron density, electrostatic potential map, Mulliken charge and local ionization potential map of NPD. The optimized geometry showed that NPD contained nitrogen as a heteroatom. The presence of nitrogen is an indication that NPD has non-bonding electrons in its molecule, which may be used for chemical bonding, thus adsorption interaction. The non-bonding electrons are possible negative charges in NPD, to corroborate this; NPD exhibited negative Mulliken charges as well as negative electrostatic charges. It showed that NPD could exhibit nucleophilic characters towards FFA. The suspected nucleophilic interaction may have taken place at the HOMO, which is the site on NPD with high electron density. This site with high electron density may serve as the active site for the nucleophilic interaction of NPD with FFA. This interaction must have resulted in the removal of FFA from WCO. The exhibited molecular properties by NPD are shown in **Table SM1**. The molecular surface area was 171.32 $Å^2$, dipole moment was 1.89 debye while solvation energy was −29.16 kJ mol^{-1}. The absolute hardness (η) was calculated as [34]:

$$\eta = \frac{E_{LUMO} - E_{HOMO}}{2} \tag{15}$$

The interaction of NPD with FFA may also be considered as a donor-acceptor interaction. The concept of donor-acceptor relationship agrees with the fact that HOMO possesses high electron density that could be donated for the interaction of NPD with FFA. Moreover, **Fig. SM4** reveals the molecular orbitals of NPD indicating electronic delocalization over nitrogen, which suggests the capacity of NPD to transfer non-bonding electrons from NPD for interaction with FFA.

Conclusion

NPD was synthesized via green chemical reaction using *n*-phenylenediamine and formaldehyde in a melt-phase process. It was characterized using FTIR, XRD, TEM, TG and EDX. NPD was applied as a useful resource for the removal of FFA in

WCO. The synthetic process gave a yield of 95%. The FTIR revealed different functional groups in NPD; the TG showed a varying mass loss at diverse temperature range while TEM revealed a smooth surface with an irregular shape. The removal of FFA from WCO may be described by pseudo-second-order with an adsorption capacity of 42.30 L kg^{-1}. The process is Langmuir isotherm favoured with ΔH of -0.679 kJ mol^{-1} and ΔS of -0.049 kJ $mol^{-1}K^{-1}$ while ΔG increased with increase in temperature. The quantum chemical analysis revealed the mechanism of removal of FFA from WCO by NPD to be via nucleophilic interaction, which may be viewed electronically as a donor-acceptor interaction. However, the current study has shown that NPD can serve as a useful resource for the removal of FFA from the waste vegetable oil.

Funding

The present work did not receive any funding

Supplementary material

SUPPLEMENTARY MATERIAL_V2.docx

Declaration of Competing Interest

All authors have read and agreed to submit this work in this journal. Authors also declare no conflict of interest.

CRediT authorship contribution statement

Titilope R. Ushedo: Resources, Formal analysis, Funding acquisition. **Olalere G Adeyemi:** Supervision, Conceptualization, Validation, Writing – original draft, Formal analysis. **Adewale Adewuyi:** Conceptualization, Supervision, Formal analysis, Writing – original draft, Software, Validation. **Woei J Lau:** Funding acquisition, Formal analysis, Writing – original draft.

Acknowledgment

First and corresponding authors are grateful to the Department of Chemical Sciences, Redeemer's University, Nigeria for provision of research space and chemicals.

Supplementary materials

Supplementary material associated with this article can be found, in the online version, at doi:10.1016/j.sciaf.2022.e01188.

References

[1] K. Jaarin, Y. Kamisah, Repeatedly heated vegetable oils and lipid peroxidation, in: A. Catala (Ed.), Lipid peroxidation, IntechOpen, 2012.
[2] R. Sayyad, Effects of deep-fat frying process on the oil quality during French fries preparation, J. Food Sci. Technol. 54 (2017) 2224–2229.
[3] A.T. Albayrak, M. Yasar, M.A. Gurkaynak, I. Gurgey, Investigation of the effects of fatty acids on the compressive strength of the concrete and the grindability of the cement, Cem. Concr. Res. 35 (2005) 400–404.
[4] W. Guo, Y. Zhu, Y. Han, Y. Wei, B. Luo, Separation mechanism of fatty acids from waste cooking oil and its flotation performance in iron ore desilicon-ization, Minerals 7 (2017) 244.
[5] H.I. Abdel-Shafy, M.S.M. Mansour, Solid waste issue: sources, composition, disposal, recycling, and valorization, Egypt. J. Pet. 27 (2018) 1275–1290.
[6] M.I. Loizides, X.I. Loizidou, D.L. Orthodoxou, D. Petsa, Circular bioeconomy in action: collection and recycling of domestic used cooking oil through a social, reverse logistics system, Recycling 4 (2019) 16.
[7] N. Ferronato, V. Torretta, Waste mismanagement in developing countries: a review of global issues, Int. J. Environ. Res. Public Health 16 (2019) 1060.
[8] U.S. Pal, R.K. Patra, N.R. Sahoo, C.K. Bakhara, M.K. Panda, Effect of refining on quality and composition of sunflower oil, J Food Sci Technol. 52 (2015) 4613–4618.
[9] X.S. Sun, in: Isolation and Processing of Plant materials. Bio-based polymers and Composites, Academic Press, 2005, pp. 33–55.
[10] R. Piloto-Rodríguez, E.A. Melo, L. Goyos-Pérez, S. Verhelst, Conversion of by-products from the vegetable oil industry into biodiesel and its use in internal combustion engines: a review, Braz. J. Chem. Eng. 31 (2014) 287–301.
[11] J. Ortega-García, N. Gámez-Meza, J.A. Noriega-Rodriguez, O. Dennis-Quiñonez, H.S. García-Galindo, J.O. Angulo-Guerrero, L.A. Medina-Juárez, Refining of high oleic safflower oil: effect on the sterols and tocopherols content, Eur. Food Res. Technol. 223 (2006) 775–779.
[12] H. Haslenda, M.Z. Jamaludin, Industry to industry by-products exchange network towards zero waste in palm oil refining processes, Resour. Conserv. Recycl. 55 (2011) 713–718.
[13] Y. Ma, L. Shi, Y. Liu, Q. Lu, Effects of neutralization, decoloration and deodorization on polycyclic aromatic hydrocarbons during laboratory-scale oil refining process, J. Chem. 2017 (2017) 1–9.
[14] S. Chumsantea, K. Aryusuk, S. Lilitchan, N. Jeyashoke, K. Krisnangkura, Reducing oil losses in alkali refining, JAOCS 89 (2012) 1913–1919.
[15] M.L.T.A. Putranti, S.K. Wirawan, I.M. Bendiyasa, Adsorption of free fatty acid (FFA) in low-grade cooking oil used activated natural zeolite as adsorbent, IOP Conf. Ser. Mater. Sci. Eng. 299 (1) (2018) 012085 IOP Publishing.
[16] W. Clowutimon, P. Kitchaiya, P. Assawasaengrat, Adsorption of free fatty acid from crude palm oil on magnesium silicate derived from rice husk, Eng. J. 15 (2011) 15–26.
[17] D.L. Manuale, G.C. Torres, J.M. Badano, C.R. Vera, J.C. Yori, Adjustment of the biodiesel free fatty acids content by means of adsorption, Energy fuels 27 (2013) 6763–6772.
[18] A. Ismaila, N.N. Saimon, M. Jusoh, Z.Y. Zakaria, Adsorption of free fatty acid in biodiesel from palm fatty acid distillate using KOH-activated starch, Chem. Eng. Trans. 56 (2017) 619–624 (2017).
[19] T.W. Chung, Y.L. Wu, S.H. Hsu, May 2018, Removal of free fatty acid from plant oil by the adsorption process, IOP Conf. Ser. Mater. Sci. Eng. 362 (2018) 012019 IOP Publishing.

[20] B.M.J. Baptiste, B.K. Daniele, E.M. Charlène, T.T.L. Canuala, E. Antoine, K. Richard, Adsorption mechanisms of pigments and free fatty acids in the discoloration of shea butter and palm oil by an acid-activated Cameroonian smectite, Sci. Afr. 9 (2020) p.e00498.
[21] D.S.P. Handoko, The improvement of waste cooking oil quality using H5-NZA adsorbent in fluid fixed bed reactor, J. ILMU DASAR. 10 (2009) 121–132.
[22] M.L.T.A. Putranti, S.K. Wirawan, I.M. Bendiyasa, Adsorption of free fatty acid (FFA) in low-grade cooking oil used activated natural zeolite as adsorbent, IOP Conf. Ser. Mater. Sci. Eng. 299 (2018) 012085.
[23] R.V. Escobedo, P.H. Luna, I.C.J. Torres, A.O. Mopreno, M.C.R. Ramirez, Physicochemical properties and fatty acid profile of eight peanut varieties grown in Mexico, CyTA J. Food 13 (2015) 300–304.
[24] H.A. Zahran, H.Z. Tawfeuk, Physicochemical properties of new peanut (*Arachis hypogaea* L.) varieties, OCL 26 (2019) 19.
[25] S. Singh, A. Singh, N. Kaur, Imine-linked receptors decorated ZnO-based dye-sensitized solar cells, Bull. Mater. Sci. 39 (2016) 1371–1379.
[26] S. Rahayu, Supriyatin, A. Bintari, Activated carbon-based bio-adsorbent for reducing free fatty acid number of cooking oil, in: Proceedings of the AIP Conference 2019, AIP Publishing LLC, 2018.
[27] N.A. Oladoja, R.O.A. Adelagun, A.L. Ahmad, E.I. Unuabonah, H.A. Bello, Preparation of magnetic, macro-reticulated cross-linked chitosan for tetracycline removal from aquatic systems, Colloids Surf. B: Biointerfaces 117 (2014) 51–59.
[28] S. Lagergren, About the theory of so-called adsorption of soluble substances, K. Sven. Vetensk. Handl. 24 (1898) 1–39.
[29] Y.A. Alhamed, Adsorption kinetics and performance of packed bed adsorber for phenol removal using activated carbon from dates' stones, J. Hazard Mater. 170 (2009) 763–770.
[30] Y.S. Ho, G. McKay, Pseudo-second order model for sorption processes, Proc. Biochem. 34 (1999) 451–465.
[31] O.A. Ekpete, M. Horsfall Jnr, A.I. Spiff, Kinetics of chlorophenol adsorption onto commercial and fluted pumpkin activated carbon in aqueous systems, Asian J. Nat. Appl. Sci. 1 (2012) 106–117.
[32] K.R. Ranjith, R.P. Hanumantha, M. Arumugam, Lipid extraction methods from microalgae: a comprehensive review, Front. Energy Res. 2 (2015) 61.
[33] A. Adewuyi, R.A. Oderinde, Chemically modified vermiculite clay: a means to removing emerging contaminant from polluted water system in developing nation, Polym. Bull. 76 (2019) 4967–4989.
[34] A. Adewuyi, A. Oluwaseyifunmi, S.S. Kaki, R.A. Oderinde, Synthesis of fatty phenylthiosemicarbazide from underutilized *Sesamum indicum* seed oil: a promising corrosion inhibitor of carbon steel in developing country, SN Appl. Sci. 1 (2019) 637.